J Math Chem (2013) 51:179–193
DOI 10.1007/s10910-012-0073-z

ORIGINAL PAPER

Measuring localization-delocalization phenomena in a quantum corral

H. H. Corzo · E. Castaño · H. G. Laguna · R. P. Sagar

Received: 3 July 2012 / Accepted: 6 August 2012 / Published online: 19 August 2012

Abstract The standard deviations and Shannon information entropies of the probability densities for a particle in a quantum corral are compared and contrasted to determine their effectiveness in measuring particle (de)localization. We illustrate how the two measures emphasize different aspects of the underlying distributions which can lead to inconsistent interpretations. Among these, we show that the Shannon entropy is able to distinguish between the presence of an attractive or repulsive effective potential in the radial Schrödinger equation while the standard deviation does not. The analysis of this radial model is then extended to momentum space where the dependence of the measures, entropic sum and uncertainty product on the effective potential, is examined.

Keywords Quantum localization-delocalization · Shannon information entropy · Quantum corral · Entropic uncertainty relation · Uncertainty product

Mathematics Subject Classification 92E99 · 94A17

H. H. Corzo · H. G. Laguna · R. P. Sagar (✉)
Departamento de Química, Universidad Autónoma Metropolitana, San Rafael Atlixco No. 186, Iztapalapa, 09340 Mexico D.F., Mexico
e-mail: sagar@xanum.uam.mx

E. Castaño
Departamento de Física, Universidad Autónoma Metropolitana, San Rafael Atlixco No. 186, Iztapalapa, 09340 Mexico D.F., Mexico

H. H. Corzo
Department of Chemistry and Biochemistry, Auburn University, Auburn, AL, 36849-5312, USA

1 Introduction

The localization-delocalization of a particle in a quantum corral is an important and relevant property in this system [1–3]. A delocalized quantum particle is one that is spread throughout the system, while a localized one is concentrated at specific site(s). The information of whether a particle is localized or delocalized lies in the specific features of its probability density.

While localization-delocalization characteristics of the particle(s) in a quantum system have become a fundamental part of current analysis, there are still some open questions: How does one know whether the system is localized or delocalized? How does one measure this (de)localization? In recent works, the standard deviation and the Shannon entropy from information theory have been used to measure (de)localization in quantum systems. Do these measures give the correct information about the (de)localization features of the quantum system? do they give consistent results or are there differences between them? is one better than the other in measuring the (de)localization present in a quantum system? We also mention that other measures have been employed to study localization in chemical systems [4].

Take for example the particle-in-a-box model. This system consists of a particle bound to the interior of a box of unit length by infinitely hard walls. In this case, the probability density for the mth eigen-state

$$\rho_{box,m}(x) = 2\sin^2(m\pi x), \tag{1}$$

has $m - 1$ nodes , as shown in Fig. 1. Therefore, the probability density tends to a uniform distribution for large quantum numbers. This is also reflected in the standard deviation of the position,

$$\Delta x_{box,m} = \frac{1}{2\sqrt{3}}\sqrt{1 - \frac{6}{\pi^2 m^2}}, \tag{2}$$

which increases with m [5].

In contrast, the Shannon entropy of this model is the same for every eigen-state, [6] with a value equal to:

$$S_{box} = -(1 - \ln 2) \simeq -0.3069, \tag{3}$$

and, therefore, does not give information about the localization of the particle in any of the eigen-states of the system.

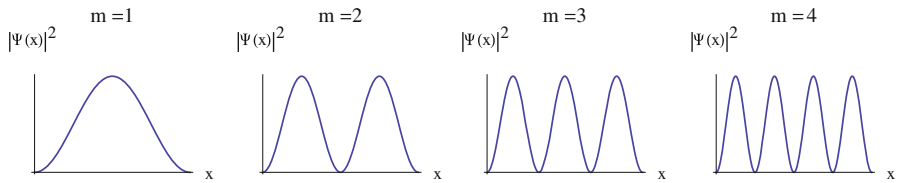

Fig. 1 Particle-in-a-box densities for the $m = 1, 2, 3, 4$ states with box length unity

1.1 Standard deviation

For many years the standard deviation has been used as a quantitative measurement of (de)localization in quantum physics. From statistics, the standard deviation of the position of a particle on the x axis is given by

$$\Delta x = (\langle x^2 \rangle - \langle x \rangle^2)^{\frac{1}{2}}, \tag{4}$$

where the moments are

$$\langle x^2 \rangle = \int \rho(x) x^2 dx, \qquad \langle x \rangle = \int \rho(x) x dx, \tag{5}$$

and the probability density $\rho(x)$ is defined in terms of the wave function of the system,

$$\rho(x) = |\Psi(x)|^2. \tag{6}$$

Smaller (larger) values of Δx are associated with a more localized (delocalized) distribution.

1.2 Shannon entropy

On the other hand, one of the most useful tools from information theory is the Shannon information entropy [7,8]. This informational entropy has been used in the studies of different quantum systems, e.g., confined particles [6,9–11], atoms [12,13], molecules [14] and quantum revival systems [15]. It is defined as

$$S = -\int \rho(x) \ln \rho(x) dx. \tag{7}$$

The Shannon entropy is a measure of (de)localization, where larger values are indicative a more delocalized density and smaller values are associated with a localized density.

As one can see, both the standard deviation and the Shannon entropy can be used as (de)localization measures. One aspect that is important to point out is that the standard deviation has a strong dependence on the shape and width of the underlying distribution. Thus, in recent years, there have been studies that discuss the inconvenience of using the standard deviation in the analysis of quantum systems [16,17].

Perhaps one of the biggest drawbacks of the standard deviation comes from the phase problem [18]. In contrast, a recent work has shown that the Shannon entropy does not possess problems associated with the phase. For two degenerate states in a cyclic box, which are phase-shifted, it was shown that the standard deviation yields different results for each state while the Shannon entropy is the same for each state [9]. Note that phase-shifting changes the nodal structure in the cyclic box while it does not alter the relative magnitude of the peaks in the density.

1.3 The model

At very low temperatures, quantum size effects dominate the behavior of electrons confined to systems whose scales are comparable to a Fermi wavelength. These effects have been observed experimentally in, for example, quantum wires or quantum waveguides, quantum dots and two-dimensional electron gases [1,2,19–24]. In these systems, the imposed reduced dimensionality in any given direction results in well defined energy states that can be observed at temperatures T low enough so that the thermal energy, $k_B T$, is much smaller than the energy difference between respective energy levels.

Quantum corrals are systems that have been experimentally realized on the surface of very clean metals where the electrons are confined to a finite region by a barrier of atoms of a different material, as studied by Crommie et al. [1,2]. The qualitative behavior of the local density of states (LDOS) in the system could be described by solutions to Schrödinger's equation for a particle in a circular hard-wall enclosure [1].

We consider a particle confined to the interior of a circle of radius unity that is centered at the origin. Using polar coordinates, r is the distance to the origin for any point inside the unit circle, and ϕ its angle measured from a given direction. As is well known, the eigen-functions are given by,

$$\psi_{nk}(r,\phi) = R_{nk}(r)\Phi_k(\phi), \tag{8}$$

where

$$R_{nk}(r) = \sqrt{\frac{2}{J^2_{|k|+1}(x_{nk})}}\, J_k(x_{nk} r), \tag{9}$$

$$\Phi_k(\phi) = \frac{1}{\sqrt{2\pi}} e^{ik\phi}, \tag{10}$$

and $n = 1, 2, 3, \ldots$, $|k| = 0, 1, 2, 3, \ldots$, J_k is a k-order Bessel function of the first kind and x_{nk} is the nth zero of this function. The energy of each of these states is equal to

$$E_{nk} = \frac{\hbar x^2_{nk}}{2m}. \tag{11}$$

The purpose of this article is to examine the (de)localization properties of a particle in a quantum corral as an example of a two-dimensional confined quantum system. Both the standard deviation and the Shannon entropy are calculated for each of its eigen-states.

Shannon entropies are reported in units of *nats* while standard deviations are given in dimensionless units since the radius of the confining region has been taken to be equal to unity. The necessary integrals were calculated numerically.

2 Results and Discussion

2.1 Radial Shannon entropy and standard deviation

In this section we focus on the behavior of the radial Shannon entropy and radial standard deviation as a function of the quantum numbers. The radial density upon integration over the angular variable yields,

$$\rho_r(r) = |R_{nk}(r)|^2. \tag{12}$$

This density leads to expressions for the radial Shannon entropy

$$S_r = -\int \rho_r(r) \ln \rho_r(r) r dr \tag{13}$$

and radial standard deviation

$$\Delta r = \left\{ \int r^2 \rho_r(r) r dr - \left[\int r \rho_r(r) r dr \right]^2 \right\}^{\frac{1}{2}}. \tag{14}$$

Figure 2 compares S_r and Δr as a function of quantum number n for selected values of quantum number k. The behavior of S_r depends on the value of k. For $k = 0-4$, S_r decreases (the density localizes) with n, while for $k > 4$, S_r increases (the density delocalizes) up to a maximum before it begins to decrease. This behavior was also observed for larger values of k.

Strikingly, the behavior of S_r is different to that of Δr. First, the interpretation of larger delocalization with n, (Δr increases) in the standard deviation is *opposite* to the tendency of localization seen in the entropy (S_r decreases for $k \leq 4$).

Second, the behavior of Δr with n is consistent for *all* values of k, unlike the case of S_r where the behavior for $k \leq 4$ is different from that of $k > 4$. This increase

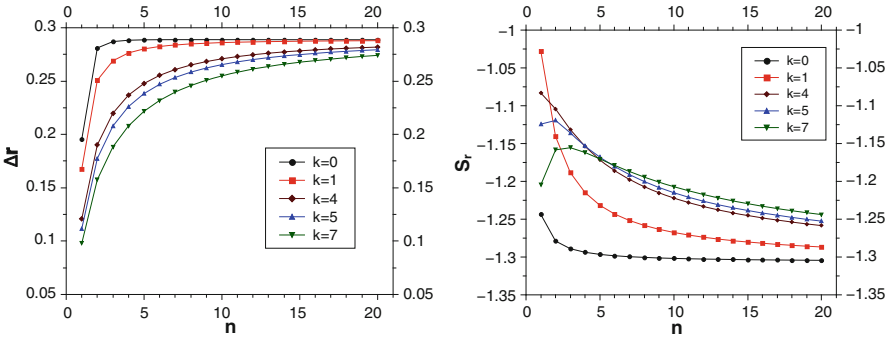

Fig. 2 Radial standard deviation (*left*) and radial Shannon entropy (*right*) as functions of the principal quantum number, n

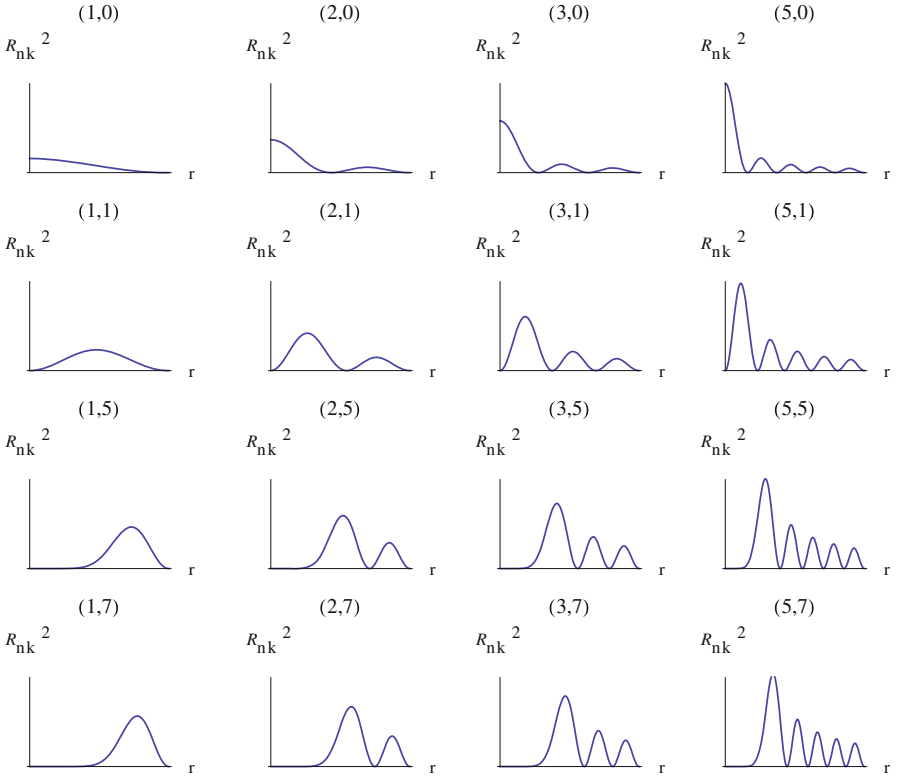

Fig. 3 Plots of the R_{nk}^2 density for states labeled as (n, k)

of Δr with n in this model is consistent with that reported for it's behavior in non-relativistic and relativistic hydrogen-like atoms as a function of principal quantum number [25,26]. Also, S_r increases with principal quantum number in spherically averaged hydrogenic orbitals [12].

The behavior of the two measures with n can be ascertained by examination of the underlying probability densities in Fig. 3. The densities for different quantum numbers (n, k) have been plotted and can be analyzed as functions of n for different values of k (rows) or as functions of k for different values of n (columns).

The standard deviation increases across rows (n) due to the presence of more nodal structure, hence the interpretation is more delocalization. In the first two rows ($k = 0, 1$), one observes that not only do the number of peaks increase (nodal structure), but the relative magnitudes among the peaks also increase (there is one which is dominant in magnitude). This is detected by the Shannon entropy as *localization* and not *delocalization* as in the case of the standard deviation.

Why does the Shannon entropy first detect delocalization for $k > 4$? That is, $S_r^{(1,5)} < S_r^{(2,5)}$, and $S_r^{(1,7)} < S_r^{(2,7)} < S_r^{(3,7)}$. It is because the first members, (1,5) and (1,7), are already localized. See for example the differences between these and (1,0) (1,1). There is a large region around the origin where the density is virtually zero in

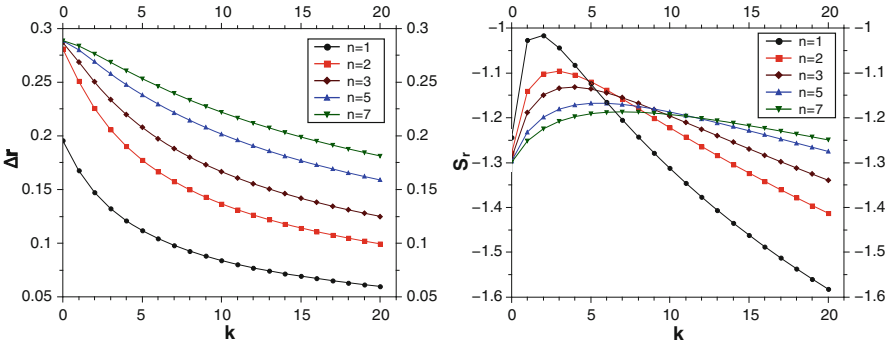

Fig. 4 Radial standard deviation (*left*) and radial Shannon entropy (*right*) as functions of the angular quantum number, k

the (1,5) and (1,7) states. The presence of more nodal structure as one goes across the third and fourth rows pushes the density inward towards the origin, resulting in delocalization. There is a point where the introduction of nodal structure does not 'push back' the density towards the origin to a large extent, and as a consequence the behavior of S_r is determined by the relative magnitudes of the peaks due to the nodal structure as in $k = 0, 1$, i.e. localization.

We present in Fig. 4 curves of Δr and S_r as functions of quantum number k for different values of n. First, Δr decreases with k for all values of n. Thus the interpretation from the standard deviation is that the density localizes. We also mention that this behavior is present for larger values of n which are not presented for brevity. This localization of the density with k can be examined by focusing on the columns of Fig. 3. The number of peaks and the nodal structure is the same throughout a particular column so this cannot be the determining factor (as in the rows). However, one does observe that density is removed from around the origin and pushed towards the boundary, which results in localization. We also mention that this behavior is consistent with that noted for the standard deviation as a function of azimuthal quantum number in the non-relativistic hydrogen-like atom [25].

Once again, the behavior of S_r is different from that of Δr. S_r first increases with k before it begins to decrease. The positions of the maxima are also seen to increase with n. The salient point here is that the behavior of both measures is consistent only for large values of k. This behavior was also observed for larger values of n. Interestingly, the behavior of S_r for small k is similar to that reported for Δr of relativistic hydrogen-like atoms as a function of small azimuthal quantum number [26].

Why does S_r first increase for smaller values of k? Figure 3 shows that the relative magnitudes of the peaks in the density become smaller which leads to delocalization. After this, the density is pushed into regions closer to the boundary, and this is the determining factor of why the density localizes (S_r and Δr both decrease). The Shannon entropy is able to capture subtle patterns in the density which are not apparent in the standard deviation.

2.2 Radial Schrödinger equation and effective potential

2.2.1 Position space

One may consider reducing the two-dimensional problem to a one-dimensional one by formulating the problem in terms of a radial Schrödinger equation. Substituting the wave function in Eq. (8) into the Schrödinger equation and operating yields,

$$-\frac{1}{r}\frac{d}{dr}\left(r\frac{dR_{nk}}{dr}\right)+\frac{k^2}{r^2}R_{nk}=\epsilon R_{nk} \tag{15}$$

where $\epsilon=\frac{2mE}{\hbar^2}$. One now defines a new variable

$$u_{nk}(r)=\sqrt{r}R_{nk}(r). \tag{16}$$

Substituting into Eq. (15) gives,

$$-\frac{d^2u_{nk}}{dr^2}+\frac{k^2-1/4}{r^2}u_{nk}=\epsilon u_{nk}. \tag{17}$$

This equation can be interpreted as a one-dimensional radial Schrödinger equation with effective potential given by

$$\frac{k^2-1/4}{r^2}. \tag{18}$$

Since the u's are zero at $r=0$ and $r=1$, this model is equivalent to the particle-in-a-box model discussed in the Introduction to this work, where the particle is now under the influence of an effective potential that is attractive towards the center of the confining region for $k=0$, while it is repulsive for all other integer values of k. The density for each eigen-state is equal to,

$$\rho_{1D}(r)=|u_{nk}(r)|^2=rR_{nk}^2(r), \tag{19}$$

and the corresponding effective Shannon entropy for the radial direction is

$$S_{1D}=-\int\rho_{1D}(r)\ln\rho_{1D}(r)dr. \tag{20}$$

Note that the the standard deviation is the same, while the expressions for S_r and S_{1D} are different. The difference is that there is a factor of r inside the logarithmic argument in S_{1D} while there is no such factor in S_r which leads to the relationship

$$S_r=S_{1D}+\int\rho_{1D}(r)\ln r dr. \tag{21}$$

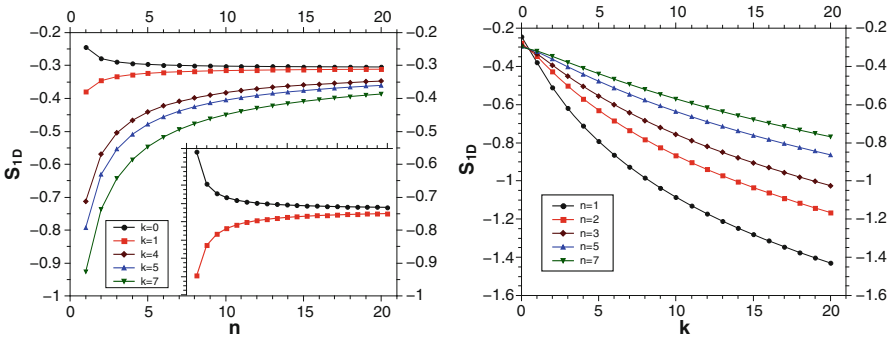

Fig. 5 S_{1D} as a function of the principal, n, (*left*) and the angular, k, (*right*) quantum numbers. The inset on the left contrasts the behavior of $k = 0$ (attractive potential) and $k = 1$ (repulsive potential)

The integral above may be defined as $\langle \ln r \rangle_{\rho_{1D}}$. Thus, any difference between the behaviors of S_r and S_{1D} must be due to this term.

The behavior of S_{1D} with n is given in Fig. 5. Notably, this behavior is now consistent with that of the standard deviation. That is, all curves increase with n as the density delocalizes. The one exception to this is $k = 0$ where there is localization (curve decreases) instead of delocalization.

Why is there a difference in the behavior of S_{1D} for $k = 0$ and $k \neq 0$? The underlying densities are plotted in Fig. 6. For $k \neq 0$, there is a repulsive potential (whose intensity increases with k) which pushes the electron away from the origin towards the boundary. Thus the first state, $n = 1$, already has a localized density. As n increases, the density is pushed back toward the origin with the introduction of a nodal structure which leads to delocalization.

For $k = 0$, there is an attractive potential which distributes the density (delocalizes) throughout the system in the $n = 1$ case, in a form more pronounced than in the particle-in-a-box case. The introduction of nodal structure and the differences in relative magnitudes of the peaks leads to localization. Most importantly, the behavior of the S_{1D} versus n curves distinguishes between the presence of an attractive or repulsive effective potential. We emphasize that the standard deviation does not detect this behavior.

Note that all curves tend towards an asymptotic limit with the curves for larger k (stronger repulsive potential) approaching this limit more slowly. We verified numerically that this asymptotic limit corresponds to the value of the particle-in-a-box model (≈ -0.3096). This is also consistent with the results for the standard deviation (Fig. 2). That is, for large n, the asymptotic value is that of the particle-in-a-box (≈ 0.2887 when $m \to \infty$).

This result may be understood in the following manner: This model has characteristics of the particle-in-a-box model plus a potential. For smaller n, S_{1D} and Δr are sensitive to the potential while for large n the nodal structure in the density dominates their behaviors and their values revert to that of the particle-in-a-box (Compare the densities in the last column of Fig. 6 with the densities in Fig. 1). The larger k curves approach the limit more slowly since the potential still dominates the behavior of the density for larger values of n.

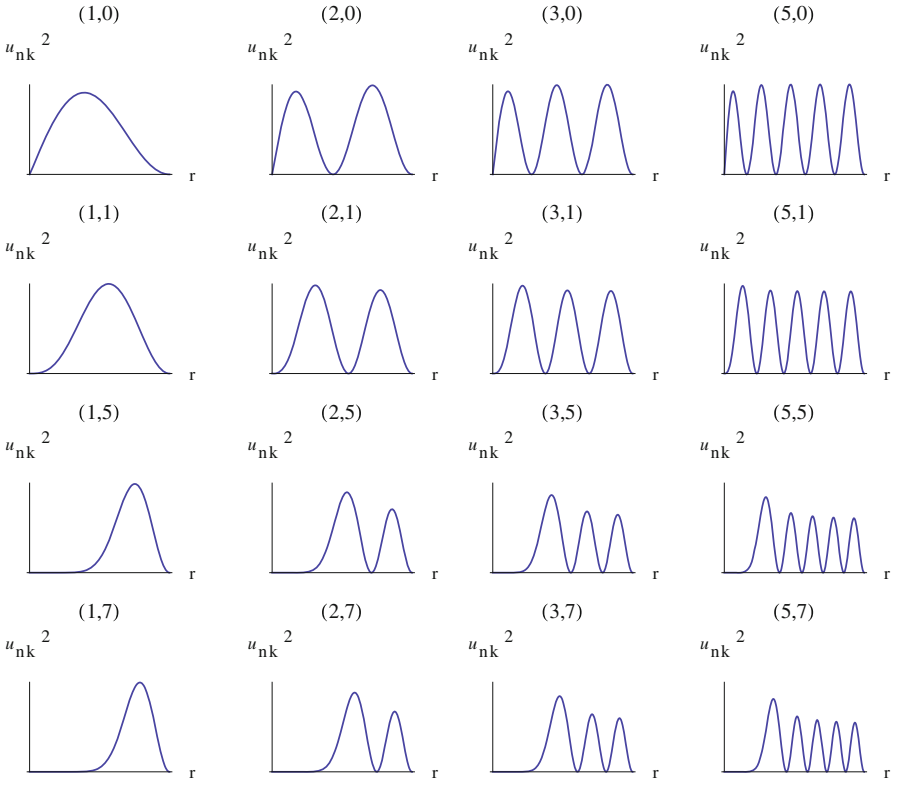

Fig. 6 Plots of the u_{nk}^2 density for states labeled as (n, k)

The dependence on the effective potential can be recovered from the standard deviation by defining the difference, $\delta = \Delta r_{nk} - \Delta x_{box,m}$, with $n = m$. This yields $\delta < 0$ for $k > 0$ which corresponds to a repulsive effective potential while $\delta > 0$ for $k = 0$ is indicative of an attractive potential.

The curves of S_{1D} versus k in Fig. 5 paint a consistent interpretation with the standard deviation. All curves decrease (localization) with k. The columns of Fig. 6 can be used to interpret these results. For $k = 0$, there is an attractive potential which distributes the density throughout the system. For $k > 0$ there is a repulsive potential which pushes the density away from the origin towards the boundary resulting in localization. Also, the strength of the repulsive potential grows with k which pushes the density further towards the boundary. Thus there is greater localization for larger k due to the larger repulsive potential.

2.2.2 Momentum space

In this section we will explore the behavior of the corresponding quantities in momentum space. Momentum space wave functions were obtained by numerical Dirac-Fourier transformation of the position space ones,

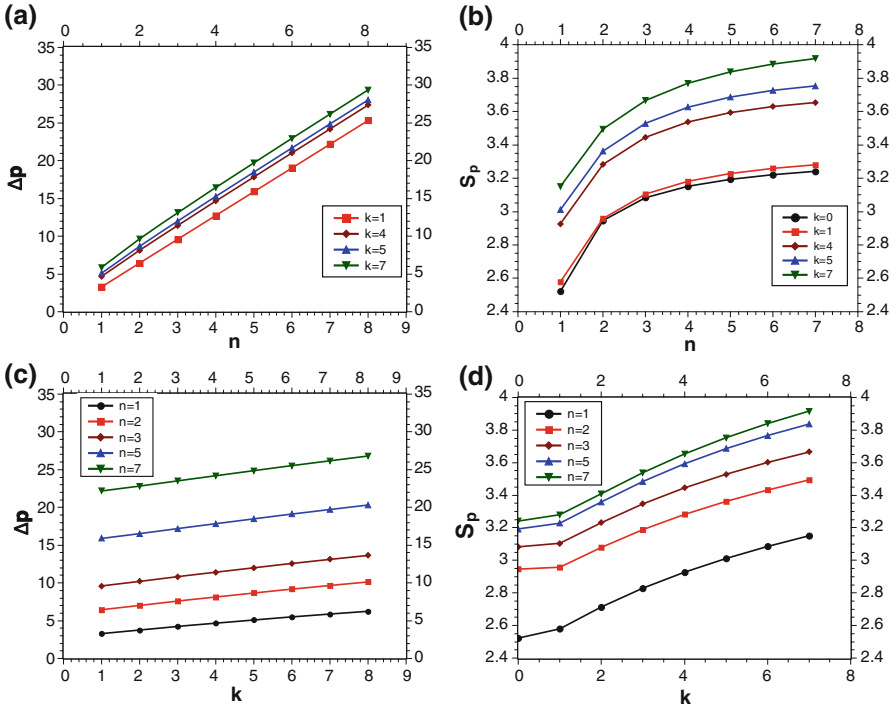

Fig. 7 Δp and S_p as functions of quantum numbers, n and k

$$t(p) = \frac{1}{\sqrt{2\pi}} \int u_{nk}(r) e^{-ipr} dr. \tag{22}$$

The momentum space Shannon entropy is defined in terms of the momentum density, $|t(p)|^2$, as

$$S_p = -\int_{-\infty}^{\infty} |t(p)|^2 \ln |t(p)|^2 dp \tag{23}$$

while the standard deviation in atomic units is

$$\Delta p = \sqrt{\langle p^2 \rangle - \langle p \rangle^2} = \left\{ -\int u_{nk}(r) \frac{d^2}{dr^2} u_{nk}(r) dr + \left[\int u_{nk}(r) \frac{d}{dr} u_{nk}(r) dr \right]^2 \right\}^{\frac{1}{2}}. \tag{24}$$

We verified numerically that $\langle p \rangle = 0$ in this model, similar to the particle-in-a-box model.

Figure 7 contrasts the behaviors of Δp and S_p as functions of n and k. As a function of n, Δp is linear while S_p is an increasing function of n. The observed linearity of Δp with n, and the behavior of S_p, is similar to the behaviors with m in the

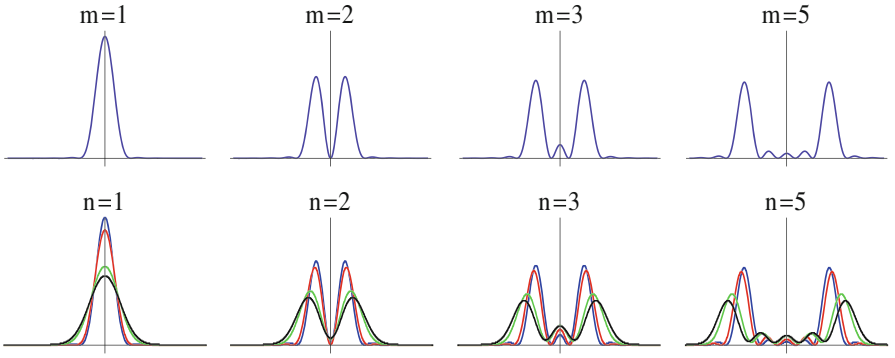

Fig. 8 Momentum densities as a function of p for selected states in the particle-in-a-box model (m) and the radial model with effective potential (n). The colors in the lower *curves* correspond to *blue* ($k = 0$), *red* ($k = 1$), *green* ($k = 5$), *black* ($k = 7$) (Color figure online)

particle-in-a-box model [27]. Notably, the behavior of S_p with n does not distinguish between attractive or repulsive potentials, as in the case of S_{1D}.

Momentum densities, along with those of the particle-in-a-box, are given in Fig. 8. One can observe similar trends in the densities of both models for a particular value of $n(m)$. With increasing n, there is more nodal structure in the densities which results in a transferral of density from around the origin, or small p, to regions of larger p. The net result is delocalization which is observed from the increasing tendencies of both Δp and S_p.

The trends noted above as functions of n are also repeated as functions of k. That is, Δp displays a linear behavior while S_p is an increasing function of k. The attractive potential ($k = 0$) has the most localized momentum space density as measured by S_p. Elevating the intensity of the repulsive potential (larger $k > 0$) delocalizes the momentum density. Note that the values for $k = 0$ are not included in the Δp plot since the integral corresponding to $\langle p^2 \rangle$ does not converge for these particular states.

These behaviors can be interpreted from the densities given in Fig. 8. Both attractive and repulsive potentials remove density from the smaller p regions and place it at larger p, resulting in a delocalization of the momentum density as compared to the particle-in-a-box. This is combined to a lesser extent with the addition of density in the small p region close to the origin (for $n > 1$). Thus pulling the position density towards the origin in position space as a result of an attractive potential, or pushing the position density towards the barrier as a result of a repulsive potential, both result in a transferral of momentum density towards larger p.

The interest in both S_{1D} and S_p is warranted since they are components of an entropic uncertainty relation [28]

$$S_t = S_{1D} + S_p \geq 1 + \ln \pi \approx 2.1447, \tag{25}$$

which may be contrasted to the one in terms of standard deviations (in atomic units)

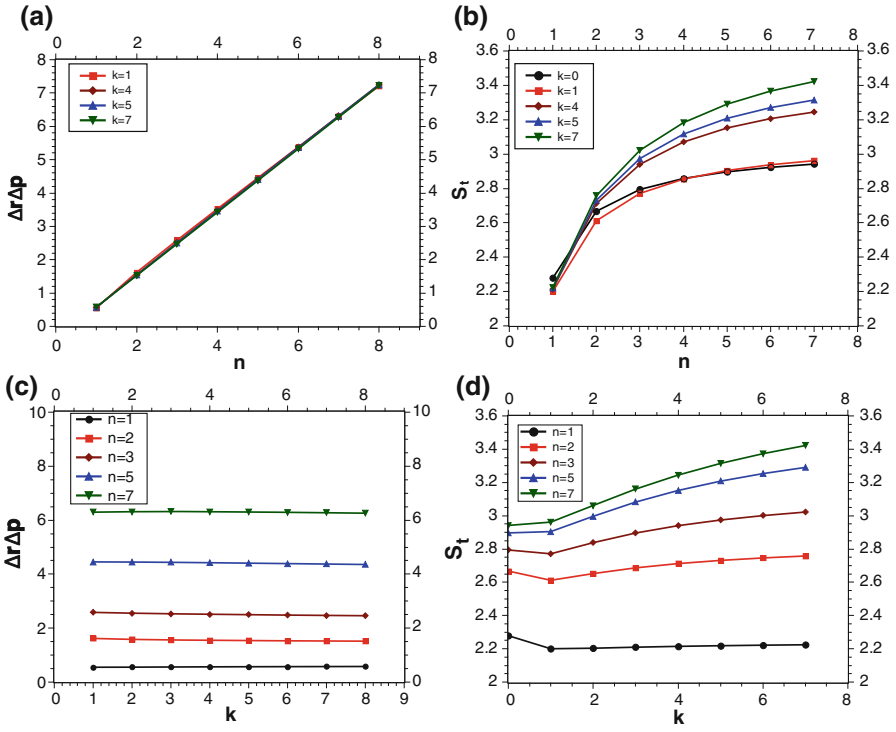

Fig. 9 $\Delta r\,\Delta p$ and S_t as functions of quantum numbers, n and k

$$\Delta r\,\Delta p \geq \frac{1}{2}. \tag{26}$$

The description of quantum fluctuations and quantum phase transitions in terms of entropic uncertainty relations have been shown to be more suitable than variance based ones [29–31].

The behavior of the entropy sum, S_t, and the uncertainty product, $\Delta r\,\Delta p$, are given in Fig. 9 as functions of n and k. With n, both the sum and the product are increasing functions, with the product exhibiting a linear behavior, analagous to the particle-in-a-box model. However, the difference is that the product does not clearly distinguish between different values of k while the sum does. This can be seen from the k dependent curves where there is more dependence on k in the entropy sum than in the product.

The entropy sum marks the difference between attractive ($k = 0$) and repulsive ($k > 0$) potentials since there is a clear change in behavior. It increases as the strength of the repulsive potential is increased. These results illustrate that the entropy sum is more sensitive to the presence and strength of the potentials as compared to the uncertainty product. We also remark that there is a crossover point in the $k = 0$ and $k = 1$ curves of S_t. This crossover point, a result of the behavior in position space

of S_{1D}, illustrates and highlights the differences between the attractive (k = 0) and repulsive (k = 1) effective potentials present in this system.

3 Conclusions

The particle in a quantum corral model is used to evaluate the standard deviation and Shannon entropy as measures of the (de)localization inherent in the underlying probability densities. Comparisons are made by analyzing the behavior of the two measures as functions of the two quantum numbers in the system. We show that this behavior is markedly different for both quantum numbers which leads to inconsistencies in interpretation. The standard deviation yields that the particle is more $delocalized$ with increasing n, independent of the value of k. On the other hand, the Shannon entropy gives that the particle is more $localized$ with increasing n, and is a result dependent on the value of k. For states with $k > 4$, the particle first delocalizes before it localizes for larger n. The standard deviation illustrates that the particle $localizes$ with increasing values of k which is consistent with the Shannon entropy, but only for larger values of k. For smaller values, the interpretation of the Shannon entropy is that the particle $delocalizes$ from one state to another. Analysis of the underlying distributions suggest that the standard deviation in this model is sensitive to the nodal structure and width of the peaks while the Shannon entropy is also sensitive to the relative magnitudes of the peaks in the distribution.

These measures are also used to examine the densities from the radial Schrödinger equation which can be considered as a model of a particle-in-a-box under the influence of an effective potential. We show that the Shannon entropy is able to distinguish between an attractive effective potential and a repulsive one as the density localizes with n for $k = 0$ (attractive) while it delocalizes with n for $k \neq 0$ (repulsive). Most importantly, the standard deviation does not distinguish between the two cases. The analysis is then extended to momentum space where we illustrate that the entropy sum is more sensitive to the presence of the potentials as compared to the uncertainty product.

Acknowledgment The authors thank the Consejo Nacional de Ciencia y Tecnología (CONACyT) for support through grant COFON 908090. HGL thanks CONACyT for a graduate fellowship.

References

1. M.F. Crommie, C.P. Lutz, D.M. Eigler, Science **262**, 218 (1993)
2. M.F. Crommie, C.P. Lutz, D.M. Eigler, Nature **363**, 524 (1993)
3. P. Roy, T.K. Ghosh, K. Bhattacharya, J. Phys. Condens. Matter. **24**, 055301 (2012)
4. J. Pipek, I. Varga, T. Nagy, Int. J. Quantum Chem. **37**, 529 (1990)
5. J. Peslak Jr, Am. J. Phys. **47**, 39 (1979)
6. V. Majerník, L. Richterek, J. Phys. A Math. Gen. **30**, L49 (1997)
7. C.E. Shannon, Bell Syst. Tech. J. **27**, 379 (1948). Reprinted in C.E. Shannon, Claude Elwood Shannon: collected papers (IEEE Press, New York, 1993)
8. T.M. Cover, J.A. Thomas, *Elements of Information Theory* (Wiley, New York, 2006)
9. H.H. Corzo, H.G. Laguna, R.P. Sagar, J. Math. Chem. **50**, 233 (2012)
10. K.D. Sen, J. Chem. Phys. **123**, 074110 (2005)

11. Á. Nagy, K.D. Sen, H.E. Montgomery Jr., Phys. Lett. A **373**, 2552 (2009)
12. S.R. Gadre, S.B. Sears, S.J. Chakravorty, R.D. Bendale, Phys. Rev. A **32**, 2602 (1985)
13. N.L. Guevara, R.P. Sagar, R.O. Esquivel, Phys. Rev. A **67**, 012507 (2003)
14. M. Ho, R.P. Sagar, D.F. Weaver, V.H. Smith Jr., Int J. Quantum Chem. **S29**, 109 (1995)
15. E. Romera, F. de Los Santos, Phys. Rev. Lett. **99**, 263601 (2007)
16. I. Bialynicki-Birula, L. Rudnicki, in *Chapter 1*, ed. by K.D. Sen Statistical Complexity, Applications in Electronic Structure (Springer, New York, 2011)
17. J. Hilgevoord, Am. J. Phys. **70**, 983 (2002)
18. J.-M. Lévy-Leblond, Ann. Phys. **101**, 319 (1976)
19. G.A. Fiete, E.J. Heller, Rev. Mod. Phys. **75**, 933 (2003)
20. E.J. Heller, Nat. Phys. **4**, 443 (2008)
21. M.F. Crommie, C.P. Lutz, D.M. Eigler, E.J. Heller, Phys. D **83**, 98 (1995)
22. K. Trivedi, H. Tuk, H.C. Floresca, M.J. Kim, W. Hu, Nano Lett. **11**, 1412 (2011)
23. J.-B. Xia, Phys. Rev. B **45**, 3593 (1992)
24. R. Di Capua, M. Radovic, G.M. De Luca, I. Maggio-Aprile, F. Miletto Granozio, N.C. Plumb, Z. Ristic, U. Scotti di Uccio, R. Vaglio, M. Salluzzo, Cond-mat/1202.0634v1 (2012)
25. C.-D. Kuo, Ann. Phys. **316**, 431 (2005)
26. W.C. Qiang, S.-H. Dong, J. Phys. A Math. Gen. **39**, 8663 (2006)
27. V. Majerník, R. Charvot, E. Majerníková, J. Phys. A Math. Gen. **32**, 2207 (1999)
28. I. Bialynicki-Birula, J. Mycielski, Commun. Math. Phys. **44**, 129 (1975)
29. E. Majerníková, V. Majerník, S. Shpyrko, Eur. Phys. J.B. **38**, 25 (2004)
30. E. Romera, M. Calixto, Á. Nagy, Eur. Phys. Lett. **97**, 20011 (2012)
31. M. Calixto, Á. Nagy, I. Paradela, E. Romera, Phys. Rev. A **85**, 053813 (2012)